Nanoelectromechanical system-integrated detector with silicon nanomechanical resonator and silicon nanochannel field effect transistor

Josef-Stefan Wenzler, Tyler Dunn, Shyamsunder Erramilli, and Pritiraj Mohanty[a)]
Department of Physics, Boston University, 590 Commonwealth Avenue, Boston, Massachusetts 02215, USA

(Received 12 February 2009; accepted 23 March 2009; published online 4 May 2009)

We demonstrate the fabrication and operation of an integrated device containing a nanoelectromechanical system and an integrated detector. This on-chip silicon nanochannel field effect transistor is used to measure the motion of a silicon nanomechanical resonator at room temperature. Furthermore, we describe the operation of the device as a silicon-based room-temperature on-chip amplifier for improved displacement detection of nanomechanical resonators. © *2009 American Institute of Physics*. [DOI: 10.1063/1.3122040]

I. INTRODUCTION

Motion sensors such as MEMS gyroscopes, accelerometers, pressure gauges, etc., have found their way into our daily lives in airplanes for stability control, cars as airbag release triggers, Wii controls, satellites, ink-jet printers, cameras, and pressure transducers to name just a few prominent examples.[1,2] In addition to finding use in numerous commercial applications, MEMS/nanoelectromechanical system (NEMS) sensors have been embraced by the research community to study fundamental problems such as synchronization, stochastic resonance, quantum mechanics, microscopy, and spintronics.[3–8] Next generation NEMS sensors require smaller device dimensions and higher frequencies, for which clever ICs are necessary in order to maximize signal size and minimize device costs, device footprint on the chip, and parasitic losses. Ideally, the IC is placed as close as possible to the sensor, on the same chip. However, integration of NEMS and associated electronic circuitry on a single chip is a challenging problem.[9–11] To date, the most sensitive integrated motion detector combines a nanomechanical resonator with a radio-frequency superconducting single electron transistor (rf-SSET) circuit over a 500×500 μm^2 area on a single chip.[6] Although this approach achieves exceptional charge sensitivity, the complicated fabrication process, complex measurement setup, and extreme operation conditions (ultralow temperatures) make it unfeasible for commercial applications.

Field effect transistors (FETs) have become one of the standard building blocks of integrated circuitry, and integration of these devices in local proximity to a nanomechanical resonator could circumvent problems such as extreme operation conditions and parasitic losses yet still lead to improved detection sensitivity of the mechanical motion. In particular, Silicon nanochannel (SiNC) FETs have been shown to exhibit high charge sensitivity at room temperature.[12] In this letter, we demonstrate highly reproducible fabrication and operation of a novel NEMS integrated detector (ID) device, consisting of a nanomechanical resonator and a novel NC field effect transistor, integrated over a 50×50 μm^2 area on a single chip. We describe how this device can be used as a highly sensitive displacement sensor without any of the apparent limitations of the rf-SSET sensor mentioned above, albeit with less sensitivity. Finally, we measure the displacement of the nanomechanical resonator using the integrated SiNC FET.

II. FABRICATION

For demonstration of our approach, all NEMSID devices in this letter contain a doubly clamped nanomechanical resonator integrated with a SiNC FET composed of source, drain, and top gate [see Fig. 1(a)]. All devices are fabricated from a standard silicon-on-insulator (SOI) wafer utilizing e-beam lithography and a series of standard nanomachining techniques.[13,14] A cross section of the device as cut through the middle of the SiNCs is shown in Fig. 1(b). The roman numerals represent the order of the fabrication process. First, we pattern and metalize the beam, excitation/detection electrodes, and drain/source electrodes (I). Typical beam dimensions are 15–22 μm in length, 200–300 nm in width, and 84–150 nm in thickness, along with a gap of 100–300 nm separating the beam and electrodes. The second layer (II) of fabrication involves creation of the SiNCs, which are carved into the device layer of the SOI wafer using a chromium mask and reactive ion etching. After removal of the chromium mask, a thin (15–30 nm) layer of insulating Al_2O_3 is deposited locally via atomic layer deposition to electrically

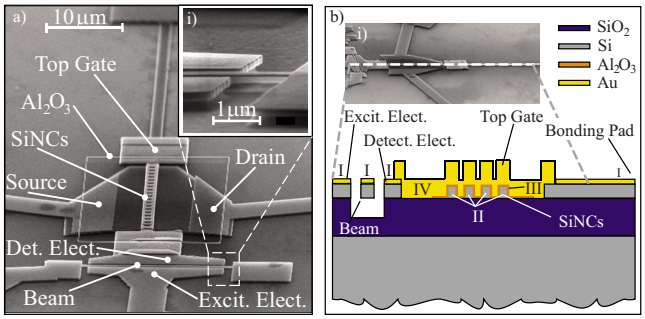

FIG. 1. (Color online) (a) Overview of the device. Inset (i) 3D image of the suspended nanomechanical beam. (b) Schematic of the cross section of the device. The roman numerals designate the order in which the device is fabricated.

[a)]Electronic mail: mohanty@bu.edu.

TABLE I. Summary of characterization of five representative NEMSID devices.

NEMS resonator				SiNC FET IC		
Sample	Dimension (μm)	f_o (MHz)	Q	SiNCs	Dimension (μm)	g_m (S)
1	l=10 w=0.3 t=0.08	19.4	600	…	…	…
2	l=20 w=0.3 t=0.08	6.3	462	1	l=1 w=0.08 t=0.08	8×10^{-7}
3	l=20 w=0.3 t=0.14	5.6	693	3	l=3 w=0.1 t=0.14	7×10^{-7}
4	l=15 w=0.3 t=0.14	8.2	1017	10	l=3 w=0.2 t=0.14	2×10^{-6}
5[a]	l=20 w=0.3 t=0.18	1.9	294	20	l=0.5 w=0.3 t=0.18	9×10^{-6}

[a]Data shown in this letter taken from sample 5.

isolate the top gate from the SiNCs (III). Each FET consists of between 1 and 20 SiNCs, each 50–500 nm wide, 0.5–6 μm long, and 80–180 nm thick. Next, a 200 nm layer of gold is deposited on top of the SiNCs forming the top gate and connecting the detection electrode with the electrode pad (IV). Finally, we suspend the beam via a hydrofluoric (HF) acid vapor etch, for demonstration, although this part of the process can also be achieved by a dry etch. We have successfully fabricated and characterized 20 of these devices with varying dimensions without compromising the quality of the SiNC FETs or the resonator. For a representative sample of these devices, see Table I.

III. EXPERIMENTAL RESULTS

We begin by testing both the beam and the SiNC FET individually. To actuate the beam, we employ a standard electrostatic technique,[15] whereby a radio-frequency voltage signal V_{in} applied to the nearby excitation electrode [see Fig. 2(a)] capacitively forces the beam. With the beam held at constant bias V_B relative to the excitation/detection electrodes, the subsequent motion of the beam induces charges on the detection electrode, which doubles as the top gate of the SiNC FET. Assuming a parallel plate capacitance C_B between the beam and the adjacent electrodes, this current can be approximated as $i_1=dQ/dt\approx\Delta Q\times f_o\approx V_B(C_B x_o/d)f_o$, where x_o is the maximum displacement of the beam, d is the equilibrium separation between the detection/excitation electrodes and the beam, f_o is the resonant frequency of the beam, and ΔQ is the charge transferred between the beam and the gate per oscillation. This current is then amplified using a transimpedance (current to voltage) amplifier [see Fig. 2(a)]. The voltage detected by the network analyzer can then be approximated as

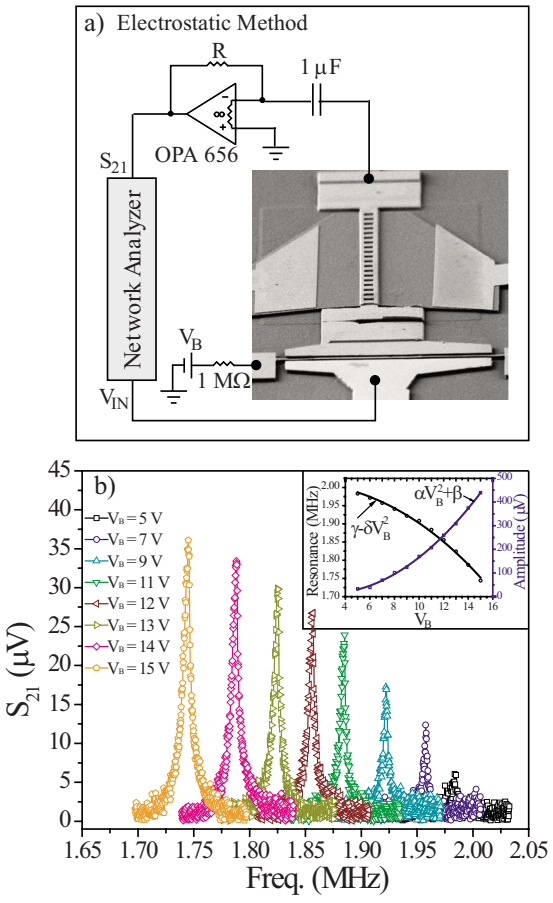

FIG. 2. (Color online) (a) Schematic of the electrostatic measurement circuit. (b) Typical response of the beam measured via the electrostatic method. Inset: Dependencies of resonance amplitude and frequency on V_B, with corresponding fits.

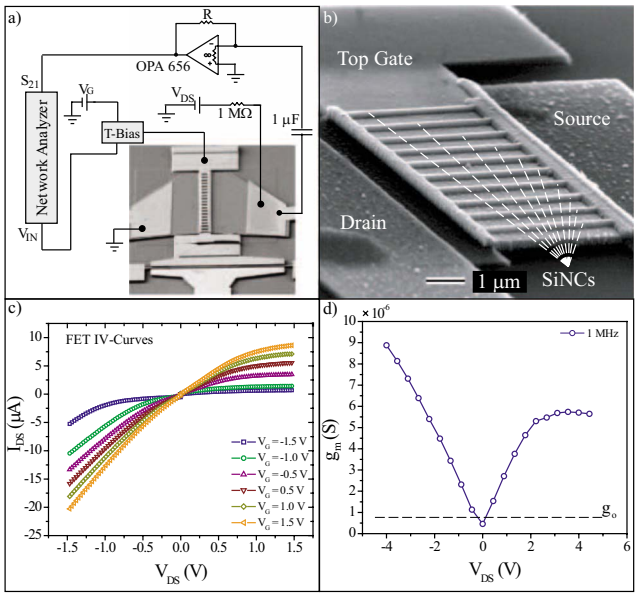

FIG. 3. (Color online) (a) Schematic of the SiNC FET characterization circuit. (b) 3D image of a SiNC FET. (c) Typical asymmetric *IV*-curves of the SiNCs. (d) Transconductance g_m of the SiNC FET for 1 MHz top gate voltage signals (V_{in}) as a function of source-drain voltage (V_G=0.5 V). The dotted line represents the minimum (unity gain) transconductance g_o required to use the SiNC FET as an amplifier at 1 MHz.

$$V_{out1} = i_1 R \approx - V_B C_B \frac{x_o}{d} f_o R, \tag{1}$$

where R is the resistor in the feedback loop of the amplifier.

Typical resonances exhibit measured amplitudes of ~100 μV and frequencies ranging from 1 to 20 MHz in good agreement with

$$f_o = 1.03 \frac{t}{l^2} \sqrt{\frac{E}{\rho}}, \tag{2}$$

a standard estimate for doubly clamped beam resonators of length l, thickness t, Young's modulus E, and density ρ.[16] The measured resonances for the beam in sample 5 (Table I) are shown in Fig. 2(b) for several different bias voltages. The inset depicts the dependencies of resonance frequency and amplitude on V_B with theoretical fits, validating that the beam survived fabrication procedures and that its operation was not compromised.[17]

We characterize the SiNC FETs, like the one seen in Fig. 3(b), by measuring their dc *IV*-curves and by determining their transconductance g_m as a function of drain-source voltage V_{DS} for 1 MHz top gate voltage signals (typical resonator frequency). The SiNC FET characterization measurement setup is depicted in Fig. 3(a). The dc *IV*-curves of the SiNC FET in sample 5 are shown for several top gate voltages V_G in Fig. 3(c). Their typical asymmetric shape[12] suggests that the SiNCs and the Al_2O_3 layer have not been damaged by the HF acid vapor etch. The dependence of the transconductance on drain-source voltage for 1 MHz top gate voltage signals is shown in Fig. 3(d) (V_G=0.5 V). As expected, the SiNC FET is most sensitive to changes in top gate voltage in the saturation region of its *IV*-curves.[17]

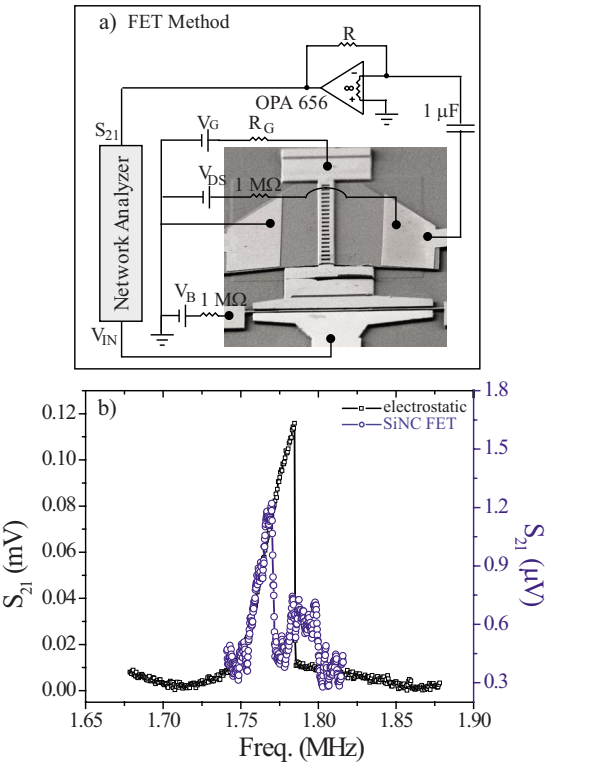

FIG. 4. (Color online) (a) Schematic of the SiNC FET motion sensor circuit. (b) Nanomechanical resonance of the beam measured using the electrostatic method (black, squares) and using the SiNC FET detection circuit (blue, circles).

Having demonstrated that neither the beam nor the SiNC FET are compromised by the fabrication procedures, we describe and attempt a room-temperature measurement of the beam resonance using the SiNC FET as a transconductance amplifier, one possible application of this integrated device. SiNC FETs are charge sensitive devices and thus ΔQ transferred between the resonating beam and the detection electrode modulates the conductance of the SiNC FET, causing a change in drain-source current.[12] This current, $i_2 = g_m(\Delta Q / C_G)$, can then be detected in exactly the same way as for the standard electrostatic method [see Fig. 4(a)], leading to an output voltage[18]

$$V_{out2} = i_2 R \approx g_m V_B \frac{x_o}{d} \frac{C_B}{C_G} R, \tag{3}$$

where g_m is the transconductance of the FET and C_G is the capacitance between the top gate and the SiNCs. Comparing Eq. (1) to Eq. (3) leads to

$$\frac{V_{out2}}{V_{out1}} = \frac{g_m}{f_o C_G}. \tag{4}$$

Thus, for this implementation, we can define the gain of the SiNC FET over the standard electrostatic measurement as $G = g_m / f_o C_G$. Therefore, as long as $G > 1$, our NEMSID device can be used as an on-chip amplifier for improved displacement detection of NEMS resonators as compared to the standard electrostatic technique. The dotted line in Fig. 3(d) represents an estimate for g_o, the transconductance leading to unity gain ($V_{out1} = V_{out2}$) at 1 MHz. By adjusting V_{DS}, we

achieve $g_m \approx 18 g_o$ signaling an amplification $G=18$ at 1 MHz. Conversely, we can view the intrinsic cut-off frequency f_T of the device to be reached when the gain of the device drops to unity[19]

$$f_T \approx \frac{g_m}{C_G}. \tag{5}$$

This frequency defines the bandwidth of the device, and it can easily be improved by enhancing the doping of the device layer to increase g_m and/or by decreasing the dimensions of the SiNCs to reduce C_G. Reasonable values for transconductance ($g_m \approx 10^{-4}$ S) and top gate capacitance ($C_G \approx 10^{-14}$) could be used to achieve a 1 GHz bandwidth.[12,13,20]

Finally, we attempt to detect the resonance of the beam via the use of the SiNC FET as depicted in Fig. 4(a). The result of this measurement (blue circles) is shown in Fig. 4(b), with the same resonance measured directly by the electrostatic method under identical drive conditions included for comparison (black squares). The resonance of the beam was detectable, demonstrating that the NEMSID device can be used as a motion sensor. However, small signal sizes measured through the SiNC FET necessitated strong driving in order to detect the resonance, leading to the asymmetric (nonlinear) shape observed. The reduced signal size is due to the electronic circuit, which was not optimized for this measurement. First, the capacitance in the detection line is dominated by parasitic contributions due to the cables and the sample stage. Second, the *RC*-circuit formed by R_G, the off-chip resistor in the top gate line as seen in Fig. 4(a) (typically megaohm), and C_{par}, parasitic capacitances in the measurement setup (typically picofarad), has a time constant of $\tau = R_G C_{\text{par}} \approx 10^{-6}$ s. Therefore, voltage buildup at the top gate is exponentially reduced for resonance frequencies $f_o \leq 1/\tau$. Both problems can be solved by micromachining a high impedance (10^8–10^9 Ω) on-chip silicon resistor along with the SiNCs, in between the top gate and the bonding pad [see Fig. 1(d)]. Such a local resistor would reduce the parasitic capacitance to 10^{-15} F, and improve the time constant $\tau = R_{\text{Si}} C_G \approx 10^{-4}$ s, allowing the SiNC FET to be used for amplification as described above. Another way to avoid signal reduction due to the measurement circuit is by adopting a nontrivial impedance matched reflection circuit to measure the change in conductance of the SiNC FET, very much like the one used by LaHaye *et al.*[6] for their rf-SSET measurement.

IV. CONCLUSION

In conclusion, we demonstrate the fabrication and operation of a novel integrated mechanical-electronic NEMSID device consisting of a nanomechanical resonator and an integrated SiNC FET. The operation of both the resonator and the SiNCs is not compromised by the integrated fabrication. We describe how this integrated device can be used as an on-chip amplifier for improved motion detection in nanomechanical structures, which under optimal conditions (higher electron mobility, shorter and wider SiNC, and higher device layer doping) could lead to a substantial signal amplification up to a bandwidth of 1 GHz. Finally, we show that the NEMSID device can be used as a motion sensor by detecting the resonance of the nanomechanical resonator through the SiNC FET.

[1] G. K. Fedder *et al.*, Proc. IEEE **96**, 306 (2008).
[2] J. J. Neumann, Jr. and K. J. Gabriel, Sens. Actuators, A **95**, 175 (2002).
[3] S. Shim, M. Imboden, and P. Mohanty, Science **316**, 95 (2007).
[4] R. Badzey and P. Mohanty, Nature (London) **437**, 995 (2005).
[5] A. Gaidarzhy, G. Zolfagharkhani, R. Badzey, and P. Mohanty, Phys. Rev. Lett. **94**, 030402 (2005).
[6] M. LaHaye, O. Buu, B. Camarota, and K. Schwab, Science **304**, 74 (2004).
[7] R. Knobel and A. Cleland, Nature (London) **424**, 291 (2003).
[8] G. Zolfagharkhani, A. Gaidarzhy, P. Degiovanni, S. Kettemann, P. Fulde, and P. Mohanty, Nat. Nanotechnol. **3**, 720 (2008).
[9] J. T. Meroño, "Integration of CMOS-MEMS resonators for radio frequency applications in VHF and UHF bands," Ph.D. thesis, 2007.
[10] F. Bannon III, J. Clark, and C. Nguyen, IEEE J. Solid-State Circuits **35**, 512 (2000).
[11] C. Nguyen, IEEE Trans. Ultrason. Ferroelectr. Freq. Control **54**, 251 (2007).
[12] Y. Chen *et al.*, Appl. Phys. Lett. **91**, 243511 (2007).
[13] Y. Cui *et al.*, Nano Lett. **3**, 149 (2003).
[14] R. Badzey, G. Zolfagharkhani, A. Gaidarzhy, and P. Mohanty, Appl. Phys. Lett. **85**, 3587 (2004).
[15] D. Guerra, M. Imboden, and P. Mohanty, Appl. Phys. Lett. **93**, 033515 (2008).
[16] M. Imboden, P. Mohanty, A. Gaidarzhy, J. Rankin, and B. Sheldon, Appl. Phys. Lett. **90**, 173502 (2007).
[17] S. Senturia, *Microsystem Design* (Kluwer Academic, Boston, MA, 2001).
[18] A. S. Sedra and K. C. Smith, *Microelectronic Circuits* (CBS College Publishing, New York, 1987).
[19] J. Guo *et al.*, IEEE Trans. Nanotechnol. **4**, 715 (2005).
[20] N. Kilchytska *et al.*, IEEE Trans. Electron Devices **50**, 577 (2003).